

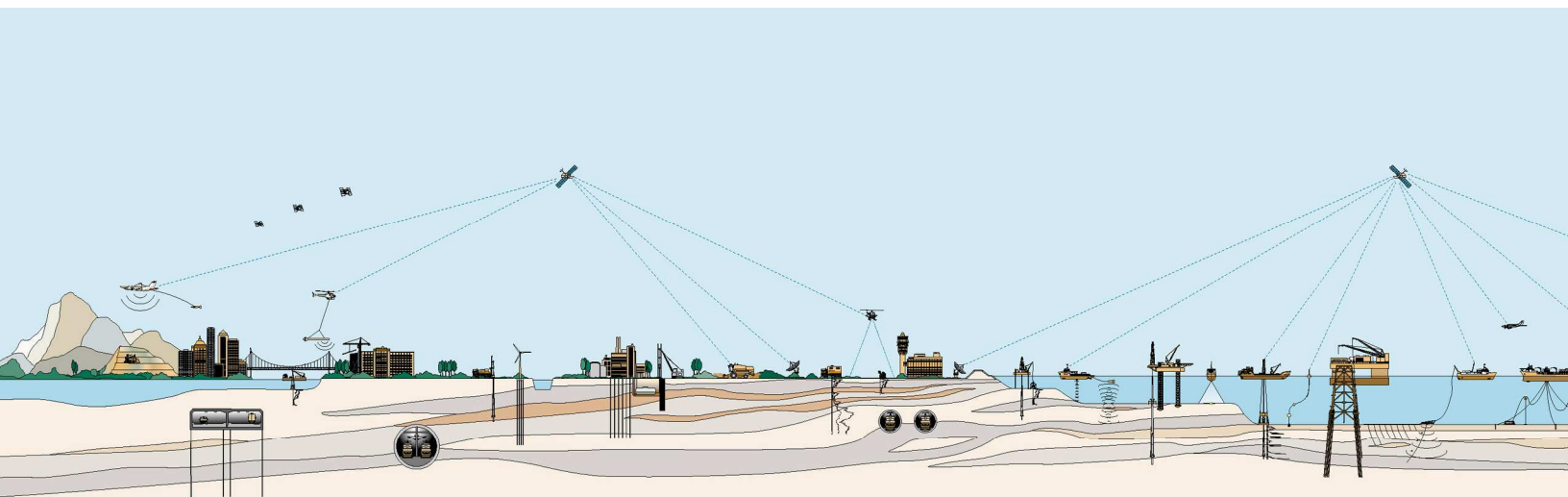


LOGISTICS AND PROCESSING REPORT
Airborne Magnetic and HELITEM[®] Survey

TENNANT CREEK AREA, NORTHERN TERRITORY, AUSTRALIA

Job No. 11012

Westgold Resources Limited





**LOGISTICS AND PROCESSING REPORT
AIRBORNE MAGNETIC AND HELITEM® SURVEY
TENNANT CREEK, NORTHERN TERRITORY,
AUSTRALIA**

JOB NO. 11012

Client: Westgold Resources Limited
Level 3, 123 Adelaide Tce, East Perth, WA 6007
Australia

Date of Report: August 31, 2011

FUGRO AIRBORNE SURVEYS

Fugro Airborne Surveys was formed in early 2000 through the global merger of leading airborne geophysical survey companies: Geotrex-Digheem, High-Sense Geophysics, and Questor of Canada; World Geoscience of Australia; Geodass and AOC of South Africa. Sial Geosciences of Canada joined the Fugro Airborne group in early 2001; Spectra Exploration Geosciences followed thereafter. In mid 2001, Fugro acquired Tesla 10 and Kevron in Australia, and certain activities of Scintrex. Fugro also works with Lasa-Geomag located in Brazil, for surveys in South America. With a staff of over 400, Fugro Airborne Surveys now operates from 12 offices worldwide.

Fugro Airborne Surveys is a professional services company specializing in low altitude remote sensing technologies and collects, processes and interprets airborne geophysical data related to the subsurface of the earth and the sea bed. The data and map products produced have been an essential element of exploration programs for the mining and oil & gas industries for over 50 years. Engineers, scientists and others with a need to map the earth's subsurface geology use Fugro Airborne Surveys for environmental and engineering solutions. From mapping kimberlite pipes and oil and gas deposits to detecting water tables and unexploded ordnance, Fugro Airborne Surveys designs systems dedicated to specific targets and survey needs. State of the art geophysical systems and techniques ensure that clients receive the highest quality survey data and images.

Fugro Airborne Surveys acquires both time domain and frequency domain electromagnetic data as well as, magnetic, radiometric and gravity data from a wide range of fixed wing (airplane) and helicopter platforms. Depending on the geophysical mapping needs of the client, Fugro Airborne Surveys can field airborne systems capable of collecting one or more of these types of data concurrently. The company offers all data acquisition, processing, interpretation and final reporting services for each survey.

Fugro Airborne Surveys is a founding member of IAGSA, the International Airborne Geophysics Safety Association. Our quality management system has successfully achieved certification to the international standard *ISO 9001:2000 Quality Management Systems - Requirements*

SUMMARY

This report describes the logistics, data acquisition, processing and presentation of results of a HELITEM® electromagnetic/magnetic survey flown from April 19, 2011 to May 11, 2011 for Westgold Resources Limited over its Tennant Creek property in Tennant Creek Area, Northern Territory, Australia. The Tennant Creek property consists of fourteen survey blocks. Total coverage of the survey blocks amounted to 1143.2 km.

The purpose of the survey was to determine the existence and locations of bedrock conductors and for better understanding of the subsurface geology within the survey areas. The EM data and the magnetic data were processed to produce images and profiles that are indicative of the magnetic and conductive properties of the survey areas. A GPS electronic navigation system ensured accurate positioning of the geophysical data with respect to the base maps.

The survey data were processed and compiled in the Fugro Airborne Surveys Toronto office. Maps and data in digital format are provided with this report.

Respectfully submitted,

FUGRO AIRBORNE SURVEYS CORP.

Stephen Carter
Geophysicist

R11012_TennantCreek

TABLE OF CONTENTS

SURVEY OPERATIONS	7
Locations of the Survey Blocks	7
System Information	11
<i>Aircraft and Geophysical On-Board Equipment</i>	12
<i>Base Station Equipment</i>	15
Survey Specifications	16
<i>Block Summary</i>	16
<i>Survey Elevation</i>	17
<i>Noise Levels</i>	17
Field Crew	18
DATA PROCESSING	19
Field	19
Flight Path Recovery	19
Altitude Data	19
Base Station Diurnal Magnetics	19
Airborne Magnetics	20
<i>Total Magnetic Intensity (TMI)</i>	20
<i>Calculated Vertical Gradient (CVG)</i>	20
Electromagnetics	20
<i>dB/dt Data</i>	20
<i>B-field Data</i>	21
<i>Coil Oscillation Correction</i>	21
<i>Stacked dB/dt Z Profiles</i>	Error! Bookmark not defined.
<i>Stacked CDT sections</i>	21
<i>Conductivity Depth Images (CDI)</i>	21
FINAL PRODUCTS	23
Digital Archives	23
Maps	23
Profile Plots	23
Report	23
Flight Path Videos	23

APPENDICES

- A HELICOPTER AIRBORNE ELECTROMAGNETIC SYSTEMS**
- B AIRBORNE TRANSIENT EM INTERPRETATION**
- C DATA ARCHIVE DESCRIPTION**
- D LIST OF PERSONNEL**

Survey Operations

Locations of the Survey Blocks

Figure 1 shows the locations of the Tennant Creek survey blocks in Tennant Creek Area, Northern Territory, Australia. The base of operations was setup at Tennant Creek. Total coverage of the blocks amounted to 1143.2 km.

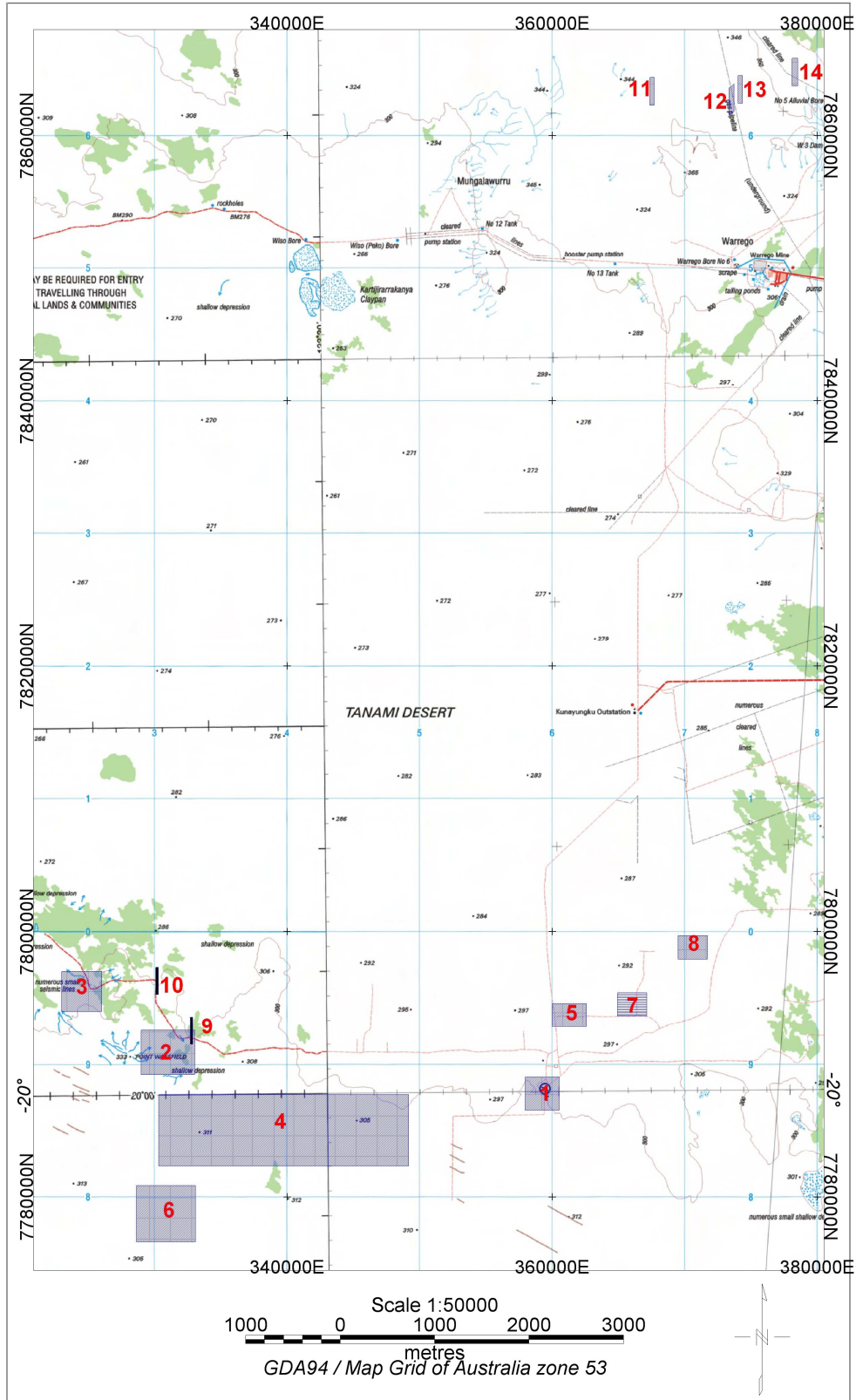


Figure 1. Survey Location.

Table 1 lists coordinates of the corner points of the survey blocks.

Block	Corners	X-UTM (E)	Y-UTM (N)
11012-1	1	357970.4	7789025.0
	2	360523.0	7789025.0
	3	360523.0	7786538.0
	4	357970.4	7786538.0
11012-2	1	329012.1	7792563.5
	2	333053.1	7792563.5
	3	333053.1	7789202.0
	4	329012.1	7789202.0
11012-3	1	323012.0	7797009.0
	2	326025.3	7797009.0
	3	326025.3	7794015.5
	4	323012.0	7794015.5
11012-4	1	330327.0	7787701.0
	2	349165.0	7787701.0
	3	349165.0	7782289.0
	4	330327.0	7782289.0
11012-5	1	360000.0	7794600.0
	2	362600.0	7794600.0
	3	362600.0	7792850.0
	4	360000.0	7792850.0
11012-6	1	328640.0	7780836.0
	2	333103.0	7780836.0
	3	333103.0	7776639.0
	4	328640.0	7776639.0
11012-7	1	364926.0	7795412.0
	2	367129.0	7795412.0
	3	367129.0	7793686.0
	4	364926.0	7793686.0
11012-8	1	369506.0	7799686.0
	2	371707.0	7799686.0
	3	371707.0	7797921.0

	4	369506.0	7797921.0
11012-9	1	332692.0	7793589.5
	2	332892.0	7793590.5
	3	332898.0	7791505.5
	4	332698.0	7791504.5
11012-10	1	330100.0	7797309.0
	2	330300.0	7797309.0
	3	330295.0	7795291.0
	4	330095.0	7795291.0
11012-11	1	367360.0	7864406.0
	2	367693.0	7864406.0
	3	367693.0	7862314.0
	4	367360.0	7862314.0
11012-12	1	373326.3	7863602.0
	2	373729.0	7863921.5
	3	373729.0	7861881.0
	4	373333.3	7861588.0
11012-13	1	374020.0	7864528.0
	2	374351.0	7864528.0
	3	374351.0	7862459.0
	4	374020.0	7862459.0
11012-14	1	378080.0	7865813.0
	2	378532.0	7865813.0
	3	378532.0	7863763.0
	4	378080.0	7863763.0

Table 1. Area Corners in UTM 53S, WGS84

System Information



Figure 2. HELITEM® System in Flight

Figure 2 depicts the HELITEM[®] system in flight. The HELITEM[®] system is composed of a 51.9 m cable to which is attached a receiver platform 22.4 m along the cable below the Helicopter, a magnetometer attached to the transmitter loop 47 m below the helicopter in flight. The top of the cable is attached to a helicopter and when in flight it drags to form a 25 degree angle from the vertical. The real time navigation GPS antenna is on the tail boom of the helicopter, the barometric altimeter, radar altimeter, video camera and data recorder are all installed in the helicopter. One GPS antenna is attached near the centre of transmitter loop to give positional information of the loop.

Aircraft and Geophysical On-Board Equipment

Aircraft:	AS 350 B3 Helicopter
Operator:	United Aero Helicopters
Registration:	VH-IPW
Survey Speed:	55 knots / 65 mph / 30 m/s
Magnetometer:	Scintrex CS-3 cesium vapour, attached to transmitter loop, sensitivity = 0.01 nT, sampling rate = 0.1 s, ambient range 20,000 to 100,000 nT. The general noise envelope was kept below 0.5 nT. The nominal sensor height was ~35 m above ground.
Electromagnetic system:	HELITEM [®] 30 channel multicoil system
Transmitter:	Vertical axis loop slung below helicopter Loop area 708 m ² Number of turns 2 Nominal height above ground 35 m
Receiver:	Multicoil system (X, Y and Z) with a final recording rate of 10 samples/second, for 30 channels of X, Y and Z component data. The nominal height above ground was ~63 m.
Base frequency:	25 Hz
Pulse width:	4 ms
Pulse delay:	0.078 ms
Off-time:	15.977 ms
Point value:	9.77 μ s
Transmitter Current:	1415 A
Dipole moment:	2x10 ⁶ Am ²

window #		Start Sample	End Sample	Number of Samples	Times from start of cycle:				Times after Tx turnoff:			
					Start Time (ms)	End Time (ms)	Width (ms)	Midpoint (ms)	Start Time (ms)	End Time (ms)	Width (ms)	Midpoint (ms)
0	Ontime	8	23	16	0.078	0.234	0.156	0.156				
1	Ontime	24	152	129	0.234	1.494	1.260	0.864				
2	Ontime	153	282	130	1.494	2.764	1.270	2.129				
3	Ontime	283	411	129	2.764	4.033	1.270	3.398				
4	Offtime	426	427	2	4.160	4.180	0.020	4.170	0.127	0.146	0.020	0.137
5	Offtime	428	430	3	4.180	4.209	0.029	4.194	0.146	0.176	0.029	0.161
6	Offtime	431	434	4	4.209	4.248	0.039	4.229	0.176	0.215	0.039	0.195
7	Offtime	435	438	4	4.248	4.287	0.039	4.268	0.215	0.254	0.039	0.234
8	Offtime	439	443	5	4.287	4.336	0.049	4.312	0.254	0.303	0.049	0.278
9	Offtime	444	449	6	4.336	4.395	0.059	4.365	0.303	0.361	0.059	0.332
10	Offtime	450	457	8	4.395	4.473	0.078	4.434	0.361	0.439	0.078	0.400
11	Offtime	458	466	9	4.473	4.561	0.088	4.517	0.439	0.527	0.088	0.483
12	Offtime	467	476	10	4.561	4.658	0.098	4.609	0.527	0.625	0.098	0.576
13	Offtime	477	489	13	4.658	4.785	0.127	4.722	0.625	0.752	0.127	0.688
14	Offtime	490	505	16	4.785	4.941	0.156	4.863	0.752	0.908	0.156	0.830
15	Offtime	506	524	19	4.941	5.127	0.186	5.034	0.908	1.094	0.186	1.001
16	Offtime	525	547	23	5.127	5.352	0.225	5.239	1.094	1.318	0.225	1.206
17	Offtime	548	575	28	5.352	5.625	0.273	5.488	1.318	1.592	0.273	1.455
18	Offtime	576	608	33	5.625	5.947	0.322	5.786	1.592	1.914	0.322	1.753
19	Offtime	609	649	41	5.947	6.348	0.400	6.147	1.914	2.314	0.400	2.114
20	Offtime	650	697	48	6.348	6.816	0.469	6.582	2.314	2.783	0.469	2.549
21	Offtime	698	756	59	6.816	7.393	0.576	7.104	2.783	3.359	0.576	3.071
22	Offtime	757	827	71	7.393	8.086	0.693	7.739	3.359	4.053	0.693	3.706
23	Offtime	828	913	86	8.086	8.926	0.840	8.506	4.053	4.893	0.840	4.473
24	Offtime	914	1016	103	8.926	9.932	1.006	9.429	4.893	5.898	1.006	5.396
25	Offtime	1017	1141	125	9.932	11.152	1.221	10.542	5.898	7.119	1.221	6.509
26	Offtime	1142	1292	151	11.152	12.627	1.475	11.890	7.119	8.594	1.475	7.856
27	Offtime	1293	1473	181	12.627	14.395	1.768	13.511	8.594	10.361	1.768	9.478
28	Offtime	1474	1693	220	14.395	16.543	2.148	15.469	10.361	12.510	2.148	11.436
29	Offtime	1694	2047	354	16.543	20.000	3.457	18.271	12.510	15.967	3.457	14.238

Table 2. HELITEM® Gate positions

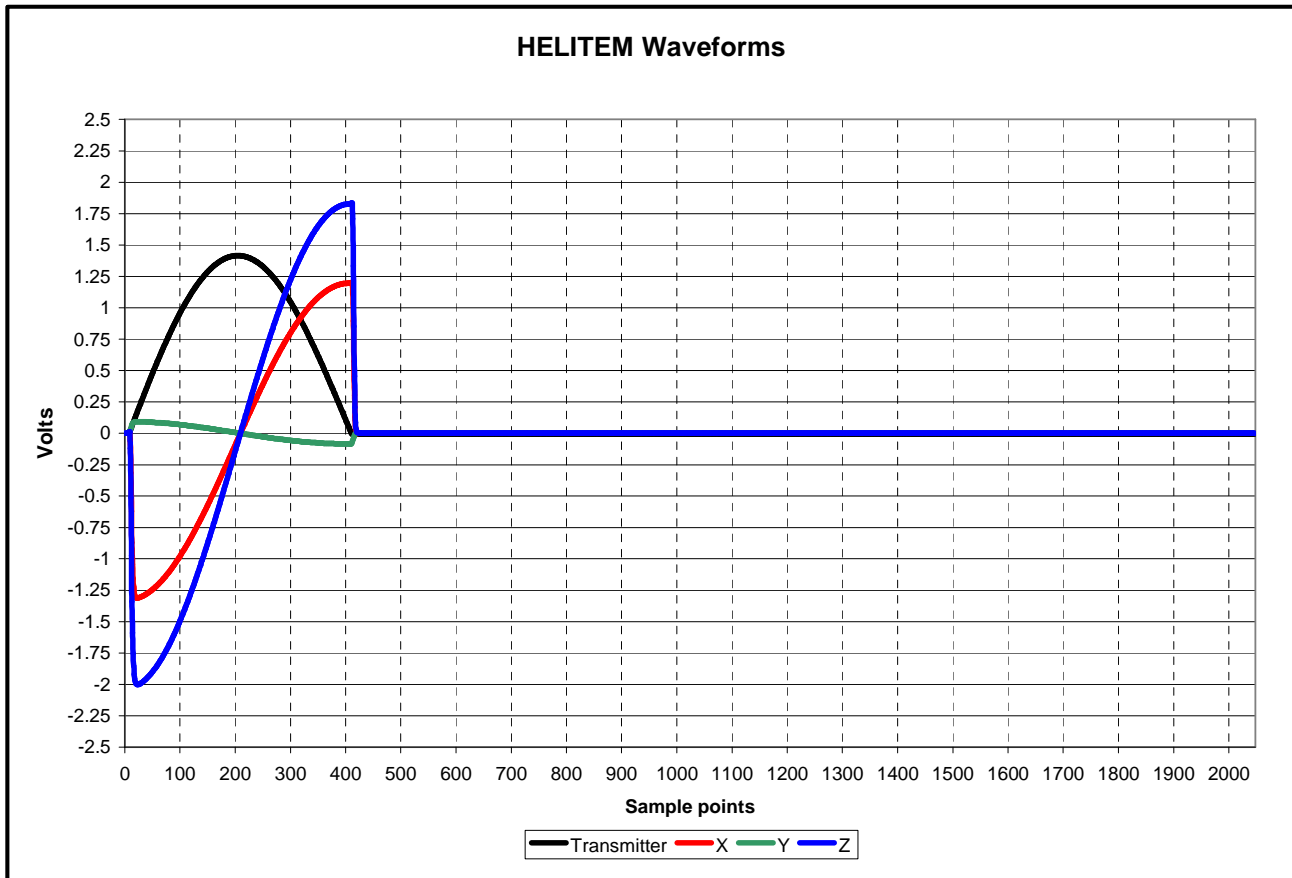


Figure 3. HELITEM® System Waveforms

Digital Acquisition:

Fugro Airborne Surveys HeliDAS system.

Barometric Altimeter:

Motorola MPX4115AP analog pressure sensor with a pressure sensitivity of 150mV/kPa and a 10 Hz sample interval, mounted in the helicopter.

Radar Altimeter:

Honeywell RT300 short pulse modulation 4.3 GHz, sensitivity 1 ft, range 0 to 2500 ft, 10 Hz recording interval mounted in the helicopter.

Camera:

Panasonic WVCD/32 Colour Video Camera

Electronic Navigation:

Novatel OEMV4/V, 0.5 sec recording interval. Antenna mounted on the tail of the helicopter.

Positional Data:

Novatel OEMV4/V, 0.5 sec recording interval. Antenna mounted on the tail of the helicopter.

Base Station Equipment

During the survey a base station GPS was set up at Tennant Creek Airport to collect data to allow post processing of the positional data for increased accuracy. The locations of the GPS base stations are recorded in Table 3

Status	Location Name	WGS84 Latitude (deg-min-sec)	WGS84 Longitude (deg-min-sec)	Orthometric Height EGM96 (m)	Date Setup	Date Torn Down
Primary	Tennant Creek Airport	19 38 25.28729 S	134 10 59.22017 E	386.778	12-Apr-11	12-May-11

Table 3. GPS Base Station Location

The magnetic base stations were setup near the GPS base stations to record diurnal data. The magnetic base station locations and base values listed are in Table 4

Status	Location Name	WGS84 Latitude (deg-min-sec)	WGS84 Longitude (deg-min-sec)	Base Level (nT)	Date Setup	Date Torn Down
Primary	Tennant Creek Airport	19 38 25.28729 S	134 10 59.22017 E	50475	12-Apr-11	12-May-11
Primary	Fuel Cache #2	19 26 19.47847 S	134 01 50.11311 E	50510	13-Apr-11	12-May-11

Table 4. Magnetic Base Station Location

GPS Novatel OEM4/V receiver system

Magnetometer Scintrex CS-2 (Primary) & CS-3 (secondary) cesium vapor sensor with timing provided by CFI Marconi GPS receiver

Survey Specifications

Block Summary

Table 5 summarizes the survey specifications for the Tennant Creek blocks, including line spacing and flight directions.

BLOCK	LINES		FLIGHT DIRECTION	LINE SPACING	PLANNED LINE km
	FROM	TO			
1	10010	10260	N-S (0°)	100 metres	65.0
	19010	19030	E-W (90°)	1000 metres	7.8
2	20010	20410	N-S (0°)	100 metres	139.4
	29010	29040	E-W (90°)	1000 metres	16.0
3	30010	30300	N-S (0°)	100 metres	90.0
	39010	39030	E-W (90°)	1000 metres	9.0
4	40010	40940	N-S (0°)	200 metres	507.6
	49010	49040	E-W (90°)	1700 metres	75.2
5	50010	50260	N-S (0°)	100 metres	46.8
	59010	59030	E-W (90°)	850 metres	7.8
6	60010	60210	E-W (90°)	200 metres	94.5
	69010	69030	N-S (0°)	2000 metres	12.6
7	70010	70120	N-S (0°)	200 metres	20.4
	79010	79020	E-W (90°)	1500 metres	4.4
8	80010	80120	N-S (0°)	200 metres	21.6
	89010	89020	E-W (90°)	1500 metres	4.4
9	90010	90010	N-S (0°)	na	2.1
10	100010	100010	N-S (0°)	na	2.0
11	110010	110020	N-S (0°)	200 metres	4.2
12	120010	120020	N-S (0°)	200 metres	4.0
13	130010	130020	N-S (0°)	200 metres	4.2
14	140010	140020	N-S (0°)	200 metres	4.2
TOTAL:					1143.2

Table 5. Summary of Survey Specification

Survey Elevation

Optimum survey elevations for the helicopter and instrumentation during normal survey flying are:

Helicopter	83 metres
HELITEM Receiver	63 metres
Magnetometer	35 metres
HELITEM Transmitter	35 metres

Survey elevations will not deviate by more than 20% over a distance of 2 km from the contracted elevation.

Survey elevation is defined as the measurement of the helicopter radar altimeter to the tallest obstacle in the helicopter path. An obstacle is any structure or object which will impede the path of the helicopter to the ground and is not limited to and includes tree canopy, towers and power lines.

Survey elevations may vary based on the pilot's judgement of safe flying conditions around man-made structures or in rugged terrain.

Noise Levels

Electromagnetic Data

The noise envelopes of the EM data, as indicated on the raw traces of dB/dt & B field channel 30 shall not exceed the following tolerances continuously over a horizontal distance of 1000 meters under normal survey conditions:

$$\text{dB/dt X and Z} < \pm 5 \text{ nT/s and B-Field X and Z} < \pm 12.5 \text{ pT.}$$

Spheric pulses may occur having strong peaks but narrow widths. The EM data are considered acceptable when their occurrence is less than 10 spheric events exceeding the stated noise specification per 100 samples continuously over a distance of 2,000 metres.

Airborne High Sensitivity Magnetometer

Magnetic total-field intensity data will be recorded on-board the aircraft as follows:

- Sample interval will be 0.1 second (10 samples/second)
- Magnetometer sensitivity will be 0.1 nT

Magnetometer noise level will not exceed ± 1.0 nT for a distance of 1 km or more.

Ground Base Station Magnetometer

Base station magnetometer information will be recorded digitally at 1.0 second intervals.

For acceptance of the magnetic data, non-linear variations in the magnetic diurnal should not exceed 10 nT over a chord of 60 seconds.

Field Crew

The field crew for the survey were as follows:

Data Processors:	Alexander Zlojutro, Stephen Carter and Shane Mule
Pilots:	Sam Bolton-Riley and Colby Tyrrell
Electronics Operators:	Matthew Higgs, Keith Lavalley, Alex Mirrilees, Tim Nykolaichuk and Jorge Naranjo

Data Processing

Field

All digital data were verified for validity and continuity. The data from the aircraft and base station were transferred to the field PC. Basic statistics were generated for each parameter recorded, these included: the minimum, maximum, and mean values; the standard deviation; and any null values located. Data were checked in the field by the FUGRO AIRBORNE SURVEYS field geophysicist for adherence to the survey specifications as outlined in the survey specifications section. Any failure to meet the survey specifications resulted in a re-flight of the line or portion of the line unless aircraft safety was at risk or the client's on site representative approved the data.

Flight Path Recovery

The quality of the GPS navigation was controlled on a daily basis by recovering the flight path of the aircraft. The correction procedure used the raw ranges from the base station to create improved models of clock error, atmospheric error and satellite orbit. These models are used to improve the conversion of aircraft raw ranges to differentially corrected aircraft position.

To check the quality of the positional data the aircraft speed is calculated using the differentially corrected x, y and z data. Any sharp changes in the speed are used to flag possible problems with the positional data. Where speed jumps occur the data are inspected to determine the source of the error. The erroneous data are deleted and splined if less than two seconds in length. If the error is greater than two seconds the raw data are examined and if acceptable may be shifted and used to replace the bad data. The gps z component is the most common source of error. When it shows problems that cannot be corrected by recalculating the differential correction the barometric altimeter is used as a guide to assist in making the appropriate correction.

Altitude Data

Radar altimeter data is de-spiked by applying a one and a half second median and smoothed using a one and a half second Hanning filter. The data are then subtracted from the GPS elevation to create a digital terrain model that is gridded and consulted in conjunction with profiles of the radar altimeter and flight path video to detect any spurious points.

Barometric altimeter data is also smoothed with a 1.5 second Hanning filter.

Base Station Diurnal Magnetics

The raw diurnal data sampled at 1 Hz are imported into a database. The data are filtered with a 5 second median filter and then a 5 second Hanning filter to remove spikes and smooth short wavelength variations. A nonlinear variation is then calculated and a flag channel is created to

indicate where the variation exceeds the survey tolerance. Acceptable diurnal data are interpolated to a 10 Hz sample rate and the local regional field value calculated from the average of the first day's diurnal data is removed to leave the diurnal variation. This diurnal variation is then ready to be used in the processing of the airborne magnetic data.

Airborne Magnetism

Total Magnetic Intensity (TMI)

The TMI data collected in flight were profiled on screen along with a fourth difference channel calculated from the TMI. Spikes were removed manually where indicated by the fourth difference. The de-spiked data were then corrected for lag by 21 samples. The diurnal variation was extracted from the filtered ground station data was then removed from the de-spiked and lagged TMI. The TMI is then tie line levelled, manually corrected and micro-levelled if necessary.

Calculated Vertical Gradient (CVG)

The first vertical derivative was calculated in the frequency domain from the final gridded TMI values to enhance subtleties related to geological structures. A first vertical derivative was gridded back to the database for display in the multi-parameter profiles.

Electromagnetics

dB/dt Data

Lag correction: 0 sample

Data correction: The X, Y and Z component data were re-processed from the raw stream to produce the 30 raw channels at 10 samples per second.

The following processing steps were applied to the dB/dt data from all coil sets:

- a) The data from channels 1 to 4 (on-time) and 5 to 30 (off-time) were corrected for drift in flight form by passing a linear fitting along each channel between the base level points selected where the pre- and post- flight background checks were conducted when the system is out of ground effect, via a graphic screen display;
- b) Both the on-time and off-time data were corrected for the noise caused by the receiver coil oscillation.
- c) Spikes caused by spherics were corrected when necessary.
- d) Noise filtering was done using an adaptive filter technique based on time domain triangular operators. Using a second difference value to identify changes in gradient along each channel, minimal filtering (21 points) is applied over the peaks of the anomalies, ranging in set increments up to a maximum amount of filtering in the resistive background areas (35 points for both the X and the Z component data);

- e) The filtered X, Y and Z component data were then levelled in flight form for any residual and nonlinear drift that was not adequately corrected during the drift correction.
- f) Line based levelling is rarely needed but is applied if necessary.

B-field Data

The processing steps for the B-field data are exactly the same as those for the dB/dt data.

Coil Oscillation Correction

The electromagnetic receiver sensor of the HELITEM® is housed in a platform container which is slung below the helicopter using a cable and attached to the transmitter loop through a network of cables. The platform design reduces the rotations of the receiver coils in flight as well as improves the stability of the receiver-transmitter geometry. However sudden changes in airspeed of the aircraft, strong variable crosswinds, or other turbulence can still result in sudden moves of the platform. This can cause the induction sensors inside the platform to rotate about their mean orientation. The rotation is most marked when the air is particularly turbulent. The changes in orientation result in variable coupling of the induction coils to the primary and secondary fields. For example, if the sensor that is normally aligned to measure the x-axis response pitches upward, it will be measuring a response that will include a mixture of the X and Z component responses. The effect of coil oscillation on the data increases as the signal from the ground (conductivity) increases and may not be noticeable when flying over areas which are generally resistive.

Using the changes in the coupling of the primary field, it is possible to estimate the pitch, roll and yaw of the receiver sensors. Only the pitch, which affects mainly the X and Z components, was considered for correction. The nominal pitch can be computed using the ideal system geometry. The pitch angles during flight are estimated and corrected to this nominal value, removing the effects caused by the deviation of the receiver sensor from its nominal position.

For the present datasets the data from all 30 channels of dB/dt and B-Field parameters have been corrected for coil oscillation.

Stacked CDT section plots

Stacked CDT section plots of every second line are presented with this report. The CDT sections were the conductivity depth imaging sections (see below) generated with EMFlow using the dB/dt Z component by Fugro Airborne Surveys Perth Office.

Conductivity Depth Images (CDI)

Conductivity Depth Imaging sections were generated from the dB/dt Z component using EMFlow by Fugro Airborne Surveys Perth office.

EMFlow was developed within the CRC-AMET through AMIRA research projects (Macnae et al, 1998, Stolz and Macnae, 1998). The software has been commercialised by Encom Technology Pty Ltd.

Conductivity values were calculated to a depth of 700m below surface at each point, using a depth increment of 5m and a conductivity range of 0.01-500mS/m.

The conductivity depth sections are created as individual grids and displayed on the multi parameter profiles. The grids have been corrected for elevation variations such that the top of each section reflects the true terrain topography. Estimated depth of penetration is also displayed on each section (the white traces).

Final Products

Digital Archives

Line and grid data in the form of Geosoft database (*.gdb) and Geosoft grids (*.grd) have been written to a DVD. The formats and layouts of these archives are further described in Appendix C (Data Archive Description). Hardcopies of all maps have been created as outlined below.

Maps

Scale: 1:20,000
Parameters: Total Magnetic Intensity
Calculated Vertical Gradient from the total magnetic intensity data
Time constant (τ)
Stacked CDT profiles
Media/Copies: PDF

Profile Plots

Scale: 1:20,000
Parameters: Multi-parameter presentation with 16 (mid to late) channels of both dB/dt and B field of X and Z component, Total Magnetic Intensity, Calculated Vertical Gradient, Radar Altimeter, Transmitter height above the EGM96 Geoid (whenever data are available), Powerline Monitor, Terrain, Helicopter height above the terrain, and Terrain adjusted CDI Sections generated with EMFlow using dB/dt Z.
Media/Copies: PDF

Report

Media/Copies: 2 paper & 1 digital (PDF format)

Flight Path Videos

Media/Copies: 5 DVDs (.Bin/BDX format)

All the grids and maps have been produced with the following coordinate system.

Projection: Universal Transverse Mercator (UTM Zone 53S)
Datum: WGS84
Central meridian: 135° East
False Easting: 500000 metres
False Northing: 0 metres
Scale factor: 0.9996

Appendix A

Helicopter Airborne Electromagnetic Systems

HELICOPTER AIRBORNE ELECTROMAGNETIC SYSTEMS

General

The operation of a helicopter time-domain electromagnetic system (EM) involves the measurement of decaying secondary electromagnetic fields induced in the ground by a series of short current pulses generated from a towed transmitter. Variations in the decay characteristics of the secondary field (sampled and displayed as windows) are analyzed and interpreted to provide information about the subsurface geology.

A number of factors combine to give the helicopter platforms good signal-to-noise ratio, depth of penetration and excellent resolution: 1) the principle of sampling the induced secondary field in the absence of the primary field (during the “off-time”), 2) the large dipole moment 3) the low flying height of the system and spatial proximity of the transmitter and receiver. Such a system is also relatively insensitive to noise due to air turbulence. However, sampling in the “on-time” can also result in excellent sensitivity for mapping very resistive features and very conductive geologic features (Annan et al, 1991, Geophysics v.61, p. 93-99).

Methodology

The Fugro time-domain helicopter electromagnetic system (HELITEM[®]) uses a high-speed digital EM receiver. The primary electromagnetic pulses are created by a series of discontinuous sinusoidal current pulses fed into a two-turn transmitting loop towed below the helicopter. The base frequency rate is selectable, with 25, 30, 75 and 90 currently being available. The length of the pulse can be tailored to suit the targets. Standard pulse widths available are 2.0 and 4.0 ms. The available off-time can be selected to be as great as 16 ms. The dipole moment depends on the pulse width and base frequency used on the survey. The specific dipole moment, waveform and gate settings for this survey are given in the main body of the report.

The receiver sensor is a three-axis (x, y & z) induction coil set housed in a platform suspended on the tow cable below the helicopter and above the transmitter. The tow cable is non-magnetic to reduce noise levels. The tow cable is 51.9 m long. The receiver is 26.7 m above and 12.9 m ahead of the transmitter in flight.

For each primary pulse a secondary magnetic field is produced by decaying eddy currents in the ground. These in turn induce a voltage in the receiver coils, which is the electromagnetic response. Good conductors decay slowly, poorer conductors more rapidly.

Operations, which are carried out in the receiver, are:

1. *Primary-field removal:* In addition to measuring the secondary response from the ground, the receiver sensor coils also measure the primary response from the transmitter. During flight, the receiver sensor position and orientation changes slightly, and this has a very strong effect on the magnitude of the total response (primary plus secondary) measured at the receiver coils. The variable primary field response is distracting because it is unrelated to the ground response. The primary field can be measured by flying at an altitude such that no ground response is measurable. These calibration signals are used to define the shape of the primary waveform. By definition this primary field includes the response of the current in the transmitter loop plus the response of any slowly decaying eddy currents induced in the

helicopter. We assume that the shape of the primary will not change as the receiver sensor position changes, but that the amplitude will vary. The primary-field-removal procedure involves solving for the amplitude of the primary field in the measured response and removing this from the total response to leave a secondary response. Note that this procedure removes any (“in-phase”) response from the ground which has the same shape as the primary field.

2. *Digital Stacking*: Stacking is carried out to reduce the effect of broadband noise in the data.
3. *Windowing of data*: The digital receiver samples the secondary and primary electromagnetic field at 2048 points per EM pulse and windows the signal in up to 30 time gates whose centres and widths are software selectable and which may be placed anywhere within or outside the transmitter pulse. This flexibility offers the advantage of arranging the gates to suit the goals of a particular survey, ensuring that the signal is appropriately sampled through its entire dynamic range.
4. *Primary Field*: The primary field at the receiver sensor is measured for each stack and recorded as a separate data channel to assess the variation in coupling between the transmitter and the receiver sensor induced by changes in system geometry.

One of the major roles of the digital receiver is to provide diagnostic information on system functions and to allow for identification of noise events, such as sferics, which may be selectively removed from the EM signal. The high digital sampling rate yields maximum resolution of the secondary field.

System Hardware

The airborne EM system consists of the helicopter, the on-board hardware, and the software packages controlling the hardware.

Transmitter System

The transmitter system drives high-current pulses of an appropriate shape and duration through the coils towed below the helicopter.

System Timing Clock

This subsystem provides appropriate timing signals to the transmitter, and also to the analog-to-digital converter, in order to produce output pulses and capture the ground response. All systems are synchronized to GPS time.

Platform Systems

A three-axis induction coil sensor is mounted inside a platform on the tow cable. The platform is connected to the transmitter loop through a network of cables to ensure a more robust and better stability of the transmitter-receiver geometry. A magnetometer sensor is attached to the transmitter loop near its centre.

Appendix B

Airborne Transient EM Interpretation

Interpretation of transient electromagnetic data

Introduction

The basis of the transient electromagnetic (EM) geophysical surveying technique relies on the premise that changes in the primary EM field produced in the transmitting loop will result in eddy currents being generated in any conductors in the ground. The eddy currents then decay to produce a secondary EM field which may be sensed in the receiver coil.

The HELITEM[®] airborne transient (or time-domain) EM system incorporates a high-speed digital receiver which records the secondary field response with a high degree of accuracy. Most often the earth's total magnetic field is recorded concurrently.

Although the approach to interpretation varies from one survey to another depending on the type of data presentation, objectives and local conditions, the following generalizations may provide the reader with some helpful background information.

The main purpose of the interpretation is to determine the probable origin of the responses detected during the survey and to suggest recommendations for further exploration. This is possible through an objective analysis of all characteristics of the different types of responses and associated magnetic anomalies, if any. If possible the airborne results are compared to other available data. Certitude is seldom reached, but a high probability is achieved in identifying the causes in most cases. One of the most difficult problems is usually the differentiation between surface conductor responses and bedrock conductor responses.

Types of Conductors

Bedrock Conductors

The different types of bedrock conductors normally encountered are the following:

1. Graphites. Graphitic horizons (including a large variety of carbonaceous rocks) occur in sedimentary formations of the Precambrian as well as in volcanic tuffs, often concentrated in shear zones. They correspond generally to long, multiple conductors lying in parallel bands. They have no magnetic expression unless associated with pyrrhotite or magnetite. Their conductivity is variable but generally high.
2. Massive sulphides. Massive sulphide deposits usually manifest themselves as short conductors of high conductivity, often with a coincident magnetic anomaly. Some massive sulphides, however, are not magnetic, others are not very conductive (discontinuous mineralization or sphalerite), and some may be located among formational conductors so that one must not be too rigid in applying the selection criteria.

In addition, there are syngenetic sulphides whose conductive pattern may be similar to that of graphitic horizons but these are generally not as prevalent as graphites.

3. Magnetite and some serpentized ultrabasics. These rocks are conductive and very magnetic.
4. Manganese oxides. This mineralization may give rise to a weak EM response.

Surficial Conductors

1. Beds of clay and alluvium, some swamps, and brackish ground water are usually poorly conductive to moderately conductive.
2. Lateritic formations, residual soils and the weathered layer of the bedrock may cause surface anomalous zones, the conductivity of which is generally low to medium but can occasionally be high. Their presence is often related to the underlying bedrock.

Cultural Conductors (Man-Made)

3. Power lines. These frequently, but not always, produce a conductive type of response. In the case when the radiated field is not removed by the power line comb filter, the anomalous response can exhibit phase changes between different windows. In the case of current induced by the EM system in a grounded wire, or steel pylon, the anomaly may look very much like a bedrock conductor.
4. Grounded fences or pipelines. These will invariably produce responses much like a bedrock conductor. Whenever they cannot be identified positively, a ground check is recommended.
5. General culture. Other localized sources such as certain buildings, bridges, irrigation systems, tailings ponds etc., may produce EM anomalies. Their instances, however, are rare and often they can be identified on the visual path recovery system.

Analysis of the Conductors

The rate of decay of a conductor is generally indicative of the conductivity of the anomalous material. However, the decay rate alone is not generally a decisive criterion in the analysis of a conductor. In particular, one should note:

- its shape and size,
- all local variations of characteristics within a conductive zone,
- any associated geophysical parameter (e.g. magnetism),
- the geological environment,
- the structural context, and
- the pattern of surrounding conductors.

The first objective of the interpretation is to classify each conductive zone according to one of the three categories which best defines its probable origin. The categories are cultural, surficial and bedrock. A second objective is to assign to each zone a priority rating as to its potential as an economic prospect.

Bedrock Conductors

This category comprises those anomalies which cannot be classified according to the criteria established for cultural and surficial responses. It is difficult to assign a universal set of values which typify bedrock conductivity because any individual zone or anomaly might exhibit some, but

not all, of these values and still be a bedrock conductor. The following criteria are considered indicative of a bedrock conductor:

1. An intermediate to high conductivity identified by a response with slow decay, with an anomalous response present in the later windows.
2. For vertical conductors, the anomaly should be narrow, relatively symmetrical, with two well-defined z-component peaks and a null between the peaks.
3. If the conductor is thin, the response characteristics varies as a function of depth and dips. If the conductor is wider, the responses might look more similar to the sphere responses.
4. A small to intermediate amplitude. Large amplitudes are normally associated with surficial conductors. The amplitude varies according to the depth of the source.
5. A degree of continuity of the EM characteristics across several lines.
6. An associated magnetic response of similar dimensions. One should note, however, that those magnetic rocks which weather to produce a conductive upper layer will possess this magnetic association. In the absence of one or more of the characteristics defined in 1, 2, 3, 4 and 5, the related magnetic response cannot be considered significant.

Most obvious bedrock conductors occur in long, relatively monotonous, sometimes multiple zones following formational strike. Graphitic material is usually the most probable source. Massive syngenetic sulphides extending for many kilometres are known in nature but, in general, they are not common. Long formational structures associated with a strong magnetic expression may be indicative of banded iron formations.

In summary, a bedrock conductor reflecting the presence of a massive sulphide would normally exhibit the following characteristics:

- a high conductivity,
- an appropriate anomaly shape,
- a small to intermediate amplitude,
- an isolated setting,
- a short strike length (in general, not exceeding one kilometre), and
- preferably, with a localized magnetic anomaly of matching dimensions.

Surficial Conductors

This term is used for geological conductors in the overburden, either glacial or residual in origin, and in the weathered layer of the bedrock. Most surficial conductors are probably caused by clay minerals. In some environments the presence of salts will contribute to the conductivity. Other possible electrolytic conductors are residual soils, swamps, brackish ground water and alluvium such as lake or river-bottom deposits, flood plains and estuaries.

Normally, most surficial materials have low to intermediate conductivity so they are not easily mistaken for highly conductive bedrock features. Also, many of them are wide and their anomaly shapes are typical of broad horizontal sheets.

When surficial conductivity is high it is usually still possible to distinguish between a horizontal plate (more likely to be surficial material) and a vertical body (more likely to be a bedrock source) thanks to the characteristic shapes of the two anomalies and the differences in the x-component responses.

One of the more ambiguous situations as to the true source of the response is when surface conductivity is related to bedrock lithology as for example, surface alteration of an underlying bedrock unit. At times, it is also difficult to distinguish between a weak conductor within the bedrock (e.g. near-massive sulphides) and a surficial source.

In the search for massive sulphides or other bedrock targets, surficial conductivity is generally considered as interference but there are situations where the interpretation of surficial-type conductors is the primary goal. When soils, weathered or altered products are conductive, and in-situ, the responses are a very useful aid to geologic mapping. Shears and faults are often identified by weak, usually narrow, anomalies.

Analysis of surficial conductivity can be used in the exploration for such features as lignite deposits, kimberlites, paleochannels and ground water. In coastal or arid areas, surficial responses may serve to define the limits of fresh, brackish and salty water.

Cultural Conductors

The majority of cultural anomalies occur along roads and are accompanied by a response on the power line monitor. This monitor is set to 50 or 60 Hz, depending on the local power grid. In some cases, the current induced in the power line results in anomalies which could be mistaken for bedrock responses. There are also some power lines which have no response whatsoever.

The power line monitor, of course, is of great assistance in identifying cultural anomalies of this type. It is important to note, however, that geological conductors in the vicinity of power lines may exhibit a weak response on the monitor because of current induction via the earth.

Fences, pipelines, communication lines, railways and other man-made conductors can give rise to responses, the strength of which will depend on the grounding of these objects.

Another facet of this analysis is the line-to-line comparison of anomaly character along suspected man-made conductors. In general, the amplitude, the rate of decay, and the anomaly width should not vary a great deal along any one conductor, except for the change in amplitude related to terrain clearance variation. A marked departure from the average response character along any given feature gives rise to the possibility of a second conductor.

In most cases a visual examination of the site will suffice to verify the presence of a man-made conductor. If a second conductor is suspected the ground check is more difficult to accomplish. The object would be to determine if there is (i) a change in the man-made construction, (ii) a difference in the grounding conditions, (iii) a second cultural source, or (iv) if there is, indeed, a geological conductor in addition to the known man-made source.

The selection of targets from within extensive (formational) belts is much more difficult than in the case of isolated conductors. Local variations in the EM characteristics, such as in the amplitude, decay, shape etc., can be used as evidence for a relatively localized occurrence. Changes in the character of the EM responses, however, may be simply reflecting differences in the conductive

formations themselves rather than indicating the presence of massive sulphides and, for this reason, the degree of confidence is reduced.

Another useful guide for identifying localized variations within formational conductors is to examine the magnetic data in map or image form. Further study of the magnetic data can reveal the presence of faults, contacts, and other features which, in turn, help define areas of potential economic interest.

Finally, once ground investigations begin, it must be remembered that the continual comparison of ground knowledge to the airborne information is an essential step in maximizing the usefulness of the airborne EM data.

Appendix C

Data Archive Description

Data Archive Description:

This archive contains data and grids of an airborne geophysical survey conducted by FUGRO AIRBORNE SURVEYS CORP for Westgold Resources Limited from April 19, 2011 to May 11, 2011 over its Tennant Creek Properties in the Northern Territory, Australia

Job # 11012

This archive comprises files in 5 directories and in the root directory:

\readme.txt - This file

GRIDS\

Grids in Geosoft format with associated .GI files

CVG_Block1.GRD -	Calculated Vertical Magnetic Gradient nT/m
CVG_Block2.GRD -	Calculated Vertical Magnetic Gradient nT/m
CVG_Block3.GRD -	Calculated Vertical Magnetic Gradient nT/m
CVG_Block4.GRD -	Calculated Vertical Magnetic Gradient nT/m
CVG_Block5.GRD -	Calculated Vertical Magnetic Gradient nT/m
CVG_Block6.GRD -	Calculated Vertical Magnetic Gradient nT/m
CVG_Block7.GRD -	Calculated Vertical Magnetic Gradient nT/m
CVG_Block8.GRD -	Calculated Vertical Magnetic Gradient nT/m

TMI_Block1.GRD -	Total Magnetic Intensity nT
TMI_Block2.GRD -	Total Magnetic Intensity nT
TMI_Block3.GRD -	Total Magnetic Intensity nT
TMI_Block4.GRD -	Total Magnetic Intensity nT
TMI_Block5.GRD -	Total Magnetic Intensity nT
TMI_Block6.GRD -	Total Magnetic Intensity nT
TMI_Block7.GRD -	Total Magnetic Intensity nT
TMI_Block8.GRD -	Total Magnetic Intensity nT

Databases\

11012_Block1_Final.GDB -	Data archive in Geosoft GDB format
11012_Block2_Final.GDB -	Data archive in Geosoft GDB format
11012_Block3_Final.GDB -	Data archive in Geosoft GDB format
11012_Block4_Final.GDB -	Data archive in Geosoft GDB format
11012_Block5_Final.GDB -	Data archive in Geosoft GDB format
11012_Block6_Final.GDB -	Data archive in Geosoft GDB format
11012_Block7_Final.GDB -	Data archive in Geosoft GDB format
11012_Block8_Final.GDB -	Data archive in Geosoft GDB format
11012_Block9_Final.GDB -	Data archive in Geosoft GDB format
11012_Block10_Final.GDB -	Data archive in Geosoft GDB format
11012_Block11_Final.GDB -	Data archive in Geosoft GDB format
11012_Block12_Final.GDB -	Data archive in Geosoft GDB format
11012_Block13_Final.GDB -	Data archive in Geosoft GDB format
11012_Block13_Final.GDB -	Data archive in Geosoft GDB format

Database_Header.txt -

Summary of line data archive

Maps\

CVG_Block1.pdf - map of Calculated Vertical Magnetic Gradient nT/m
 CVG_Block2.pdf - map of Calculated Vertical Magnetic Gradient nT/m
 CVG_Block3.pdf - map of Calculated Vertical Magnetic Gradient nT/m
 CVG_Block4.pdf - map of Calculated Vertical Magnetic Gradient nT/m
 CVG_Block5.pdf - map of Calculated Vertical Magnetic Gradient nT/m
 CVG_Block6.pdf - map of Calculated Vertical Magnetic Gradient nT/m
 CVG_Block7.pdf - map of Calculated Vertical Magnetic Gradient nT/m
 CVG_Block8.pdf - map of Calculated Vertical Magnetic Gradient nT/m

TMI_Block1.pdf - map of Total Magnetic Intensity nT
 TMI_Block2.pdf - map of Total Magnetic Intensity nT
 TMI_Block3.pdf - map of Total Magnetic Intensity nT
 TMI_Block4.pdf - map of Total Magnetic Intensity nT
 TMI_Block5.pdf - map of Total Magnetic Intensity nT
 TMI_Block6.pdf - map of Total Magnetic Intensity nT
 TMI_Block7.pdf - map of Total Magnetic Intensity nT
 TMI_Block8.pdf - map of Total Magnetic Intensity nT

Stacked_CDT_Block1.pdf - Stacked CDT sections *
 Stacked_CDT_Block2.pdf - Stacked CDT sections *
 Stacked_CDT_Block3.pdf - Stacked CDT sections *
 Stacked_CDT_Block4.pdf - Stacked CDT sections *
 Stacked_CDT_Block5.pdf - Stacked CDT sections *
 Stacked_CDT_Block6.pdf - Stacked CDT sections *
 Stacked_CDT_Block7.pdf - Stacked CDT sections *
 Stacked_CDT_Block8.pdf - Stacked CDT sections *
 Stacked_CDT_Block9.pdf - Stacked CDT sections *
 Stacked_CDT_Block10.pdf - Stacked CDT sections *
 Stacked_CDT_Block11.pdf - Stacked CDT sections *
 Stacked_CDT_Block12.pdf - Stacked CDT sections *
 Stacked_CDT_Block13.pdf - Stacked CDT sections *
 Stacked_CDT_Block14.pdf - Stacked CDT sections *

Early_Tau_Block1.pdf - Early time constant map **
 Mid_Tau_Block1.pdf - Mid time constant map **
 Late_Tau_Block1.pdf - Late time constant map **
 Early_Tau_Block2.pdf - Early time constant map **
 Mid_Tau_Block2.pdf - Mid time constant map **
 Late_Tau_Block2.pdf - Late time constant map **
 Early_Tau_Block3.pdf - Early time constant map **
 Mid_Tau_Block3.pdf - Mid time constant map **
 Late_Tau_Block3.pdf - Late time constant map **
 Early_Tau_Block4.pdf - Early time constant map **
 Mid_Tau_Block4.pdf - Mid time constant map **
 Late_Tau_Block4.pdf - Late time constant map **
 Early_Tau_Block5.pdf - Early time constant map **

Mid_Tau_Block5.pdf -	Mid time constant map **
Late_Tau_Block5.pdf -	Late time constant map **
Early_Tau_Block6.pdf -	Early time constant map **
Mid_Tau_Block6.pdf -	Mid time constant map **
Late_Tau_Block6.pdf -	Late time constant map **
Early_Tau_Block7.pdf -	Early time constant map **
Mid_Tau_Block7.pdf -	Mid time constant map **
Late_Tau_Block7.pdf -	Late time constant map **
Early_Tau_Block8.pdf -	Early time constant map **
Mid_Tau_Block8.pdf -	Mid time constant map **
Late_Tau_Block8.pdf -	Late time constant map **

Note: * CDT from EMFlow using dB/dt Z component

** Time constants generated from early, mid and late dB/dt Z windows

Profiles

Multiplots_Block1_LINE.pdf -	multi parameter profiles in PDF format
Multiplots_Block2_LINE.pdf -	multi parameter profiles in PDF format
Multiplots_Block3_LINE.pdf -	multi parameter profiles in PDF format
Multiplots_Block4_LINE.pdf -	multi parameter profiles in PDF format
Multiplots_Block5_LINE.pdf -	multi parameter profiles in PDF format
Multiplots_Block6_LINE.pdf -	multi parameter profiles in PDF format
Multiplots_Block7_LINE.pdf -	multi parameter profiles in PDF format
Multiplots_Block8_LINE.pdf -	multi parameter profiles in PDF format
Multiplots_Block9_LINE.pdf -	multi parameter profiles in PDF format
Multiplots_Block10_LINE.pdf -	multi parameter profiles in PDF format
Multiplots_Block11_LINE.pdf -	multi parameter profiles in PDF format
Multiplots_Block12_LINE.pdf -	multi parameter profiles in PDF format
Multiplots_Block13_LINE.pdf -	multi parameter profiles in PDF format
Multiplots_Block14_LINE.pdf -	multi parameter profiles in PDF format

Where LINE denotes the line number

REPORT\

R11012_Westgold.PDF -	Logistics Report
-----------------------	------------------

Database Header Information

 Project # : 11012
 Type of Survey: Fugro HELITEM and magnetic Survey
 Client: Westgold Resources Limited.
 Area: Tennant Creek, Northern Territory, Australia

 Survey Data Format

# Channel	Time	Units	Description
1 x_heli_wgs84	0.1	m	helicopter easting WGS84 (UTM Zone 53S)
2 y_heli_wgs84	0.1	m	helicopter northing WGS84 (UTM Zone 53S)
3 x_heli_gda94	0.1	m	helicopter easting GDA94 (UTM Zone 53S)
4 y_heli_gda94	0.1	m	helicopter northing GDA94 (UTM Zone 53S)
5 fid	0.1		fiducial increment
6 latitude_heli	0.1	degrees	helicopter latitude WGS 84
7 longitude_heli	0.1	degrees	helicopter longitude WGS 84
8 x_tx_wgs84	0.1	m	transmitter loop easting WGS84 (UTM Zone 53S)
9 y_tx_wgs84	0.1	m	transmitter loop northing WGS84 (UTM Zone 53S)
10 x_tx_gda94	0.1	m	transmitter loop easting GDA94 (UTM Zone 53S)
11 y_tx_gda94	0.1	m	transmitter loop northing GDA94 (UTM Zone 53S)
12 latitude_tx	0.1	degrees	transmitter loop latitude WGS 84
13 longitude_tx	0.1	degrees	transmitter loop longitude WGS 84
14 flight	0.1		flight number
15 date	0.1		flight date (yyyymmdd)
16 altrad	0.1	m	height above surface from radar altimeter
17 gpsz_heli	0.1	m	helicopter height above Geoid (EGM96)
18 gpsz_tx	0.1	m	transmitter height above Geoid (EGM96)
19 dtm	0.1	m	digital terrain model (above EGM96 Geoid)
20 diurnal	1.0	nT	measured diurnal ground magnetic intensity
21 diurnal_cor	0.1	nT	diurnal correction - base removed
22 mag_raw	0.1	nT	total magnetic intensity - spike rejected
23 mag_lag	0.1	nT	total magnetic intensity - corrected for lag
24 mag_diu	0.1	nT	total magnetic intensity - diurnal variation removed
25 tmi	0.1	nT	total magnetic intensity
26 cvg	0.1	nT/m	calculated Vertical gradient from total magnetic intensity
27 x_db_filt	0.1	nT/s	dB/dt X component channels 1 - 30 - unlevelled
28 y_db_filt	0.1	nT/s	dB/dt Y component channels 1 - 30 - unlevelled
29 Z_db_filt	0.1	nT/s	dB/dt Z component channels 1 - 30 - unlevelled
30 x_bf_filt	0.1	pT	B field X component channels 1 - 30 - unlevelled
31 y_bf_filt	0.1	pT	B field Y component channels 1 - 30 - unlevelled
32 Z_bf_filt	0.1	pT	B field Z component channels 1 - 30 - unlevelled
33 x_db_levl	0.1	nT/s	dB/dt X component channels 1 - 30 - levelled
34 y_db_levl	0.1	nT/s	dB/dt Y component channels 1 - 30 - levelled
35 Z_db_levl	0.1	nT/s	dB/dt Z component channels 1 - 30 - levelled
36 x_bf_levl	0.1	pT	B field X component channels 1 - 30 - levelled
37 y_bf_levl	0.1	pT	B field Y component channels 1 - 30 - levelled
38 Z_bf_levl	0.1	pT	B field Z component channels 1 - 30 - levelled
39 x_db_ff	0.1	nT/s/m	dB/dt Fraser Filtered X component channels 1 - 30

40 x_bf_ff	0.1	pT/m	B Field Fraser Filtered X component channels 1 – 30
41 DiffCond_db_Z	0.1	mS/m	Differential conductivity section array (5 m thickness, up to 700m) dB/dt Z
42 DiffCond_bf_Z	0.1	mS/m	Differential conductivity section array (5 m thickness, up to 700m) B Field Z
43 z_db_emflow_cdt	0.1	mS/m	EMFlow conductivity section array (5 m thickness, up to 700m), dB/dt Z
44 Powerline	0.1	uV	power line monitor channel
45 tx_current	0.1	A	transmitter peak current

Datum	WGS84
Spheroid	WGS84
Projection	UTM
Central meridian	147 East (53S)
False easting	500000
False northing	0
Scale factor	0.9996
Northern parallel	N/A
Base parallel	N/A

Appendix D

LIST OF PERSONNEL

The following personnel were involved in the acquisition, processing, and presentation of data, relating to the HELITEM® airborne geophysical survey carried out over the Tennant Creek area in Northern Territory, Australia.

David Miles	Manager, Helicopter Operations
Graham Konieczny	Manager, Data Processing and Interpretation
Lesley Minty	Project manager
Matthew Higgs	Equipment operator (FASP)
Keith Lavalley	Equipment operator (FASP)
Alex Mirrilees	Equipment operator (FASP)
Alexander Zlojutro	Field data processor (FAST)
Tim Nykolaichuk	Field data processor (FAST)
Jorge Naranjo	Field data processor (FAST)
Stephen Carter	Geophysicist, processing/EMFlow CDT (FASP)
Sam Bolton-Riley	Pilot (United Aero Helicopters)
Colby Tyrrell	Pilot (United Aero Helicopters)
Tianyou Chen	Geophysicist, processing
Lyn Vanderstarren	Drafting Supervisor
Albina Tonello	Office secretary and expeditor
Susan Pothiah	Word Processing Operator

All personnel are employees of Fugro Airborne Surveys, except for the pilots who are employees of United Aero Helicopters.